



Ignition of a lean PRF/air mixture under RCCI/SCCI conditions: A comparative DNS study

Minh Bau Luong^a, Gwang Hyeon Yu^a, Suk Ho Chung^b,
Chun Sang Yoo^{a,c,*}

^a Department of Mechanical Engineering, Ulsan National Institute of Science and Technology, Ulsan 689–798, Republic of Korea

^b Clean Combustion Research Center, King Abdullah University of Science and Technology, Thuwal, Saudi Arabia

^c School of Mechanical and Nuclear Engineering, Ulsan National Institute of Science and Technology, Ulsan 689–798, Republic of Korea

Received 2 December 2015; accepted 15 August 2016

Available online 7 October 2016

Abstract

The ignition characteristics of a lean primary reference fuel (PRF)/air mixture under reactivity controlled compression ignition (RCCI) and stratified charge compression ignition (SCCI) conditions are investigated using 2-D direct numerical simulations (DNSs) with a 116-species reduced mechanism of PRF oxidation. For RCCI combustion, *n*-heptane and *iso*-octane are used as two different reactivity fuels and the corresponding global PRF number is PRF50 which is also used as a single fuel for SCCI combustion. The 2-D DNSs of RCCI/SCCI combustion are performed by varying degree of fuel stratification, r , and turbulence intensity, u' , at different initial mean temperature, T_0 , with negatively-correlated $T-r$ fields. It is found that in the low- and intermediate-temperature regimes, the overall combustion of RCCI cases occurs earlier and its mean heat release rate (HRR) is more distributed over time than those of the corresponding SCCI cases. This is because PRF number stratification, PRF' , plays a dominant role and T' has a negligible effect on the overall combustion within the negative temperature coefficient (NTC) regime. In the high-temperature regime, however, the difference between RCCI and SCCI combustion becomes marginal because the ignition of the PRF/air mixture is highly-sensitive to T' rather than PRF' and ϕ' . The Damköhler number analysis verifies that the mean HRR is more distributed over time with increasing r because the portion of deflagration mode of combustion becomes larger with increasing fuel stratification. Finally, it is found that the overall combustion of

* Corresponding author at: Department of Mechanical Engineering, Ulsan National Institute of Science and Technology, Ulsan 44919, Republic of Korea. Fax: +82522172409.

E-mail addresses: csyoo@unist.ac.kr, withspring@gmail.com (C.S. Yoo).

both RCCI and SCCI cases becomes more like the 0-D ignition with increasing u' due to the homogenization of initial mixture by turbulent mixing.

© 2016 The Combustion Institute. Published by Elsevier Inc. All rights reserved.

Keywords: Direct numerical simulation (DNS); Homogeneous charge compression ignition (HCCI); Reactivity controlled compression ignition (RCCI); Stratified charge compression ignition (SCCI); Negative temperature coefficient (NTC)

1. Introduction

Over the past two decades, it has been demonstrated that homogeneous-charge compression ignition (HCCI) engines can provide higher thermal efficiency and lower pollutant emissions than the conventional diesel and gasoline engines [1–5]. Despite their promising advantages, however, the development of prototype HCCI engines has not been successful due to difficulties in controlling pressure rise rate (PRR) and ignition timing under high-load conditions. Therefore, several variants of HCCI engines have been proposed to enhance the ignition timing control and to extend the engine operation range. Especially, reactivity-controlled compression ignition (RCCI) and stratified-charge compression ignition (SCCI) engines have been paid considerable attention by the engine community due to their better controlling of combustion-phasing/PRR, and lower fuel consumption/pollutant emissions than the conventional HCCI engines [1,6–8].

Numerous experimental and computational studies of RCCI and/or SCCI combustion have been conducted [1,6–18]. Especially, Kokjohn et al. numerically investigated the combustion characteristics of diesel low temperature combustion (LTC), ethanol-diesel RCCI, and E85-diesel RCCI combustion. It was found that E85-diesel RCCI combustion exhibited a staged consumption of high reactive diesel and low reactive E85, and E85 is not consumed until gradual transition of diesel consumption to the second-stage ignition [9]. Kokjohn et al. also found that under RCCI conditions with either too early or too late injections of *n*-heptane, fuel/air mixture ignites nearly volumetrically due to similar ignition delays of the mixture, resulting in rapid energy release and excessive PRR [10].

Recently, it was also found from an experiment and numerical study of RCCI combustion [11] that the PRF number stratification (i.e., the reactivity stratification) plays a predominant role in controlling the overall combustion process compared to equivalence ratio stratification, while the effect of temperature stratification is negligible because the initial mean temperature, T_0 , lies within the negative temperature coefficient (NTC) regime. However, the predominant role of reactivity stratification may not remain the same when T_0 lies in

low- and high-temperature regimes, and hence, the effect of T_0 relative to the NTC regime on the RCCI combustion is still needed. Furthermore, the fundamental understanding of RCCI combustion is still limited by the capability of RANS-based simulations.

From a series of 2-D direct numerical simulation (DNS) studies of HCCI combustion [5,16,17,19–22], it was found that the ignition characteristics of two-stage ignition fuels relevant to HCCI and SCCI combustion can be significantly changed with (1) different T_0 , and (2) different levels of temperature and equivalence ratio fluctuations (T' and/or ϕ'). It was also found that (1) ϕ' becomes dominant over T' in reducing the peak of heat release rate (HRR) when T_0 lies near/within the NTC regime and, (2) T_0 in the NTC regime together with a negative T - ϕ distribution has a synergistic effect on advancing the overall combustion and smoothing out PRR and HRR under high-load SCCI combustion. It is believed that T_0 in the NTC regime also has a positive effect on enhancing the overall RCCI combustion process.

More recently, Bhagatwala et al. [18] investigated the combustion modes under RCCI conditions using DNSs with a compression heating model. They found that higher *n*-heptane concentration provides a greater degree of flame propagation; the combustion occurs in a large fraction of deflagration mode at low-to-medium pressures; the fraction of deflagration, however, is reduced with increasing pressure. It was also found from several 2-D DNS studies [5,16,19,20,22] that high turbulent mixing generally retards the overall HCCI and SCCI combustion by homogenizing the initial stratified mixture except for some HCCI combustion with very large fluctuations, resulting in high peak HRR due to dominant spontaneous ignition mode. The understanding of the effect of turbulent mixing and deflagration on the RCCI combustion, however, is still limited.

Therefore, the objective of the present study is to compare the ignition characteristics of primary reference fuel (PRF)/air mixtures under RCCI and SCCI conditions using 2-D DNSs by varying three key parameters: (1) initial mean temperature, (2) level of fuel stratification, and (3) turbulent time scale such that the relative roles of reactivity,

equivalence ratio, and temperature stratification under various conditions can be examined.

2. Numerical method and initial conditions

The Sandia DNS code, S3D, was used to solve the compressible Navier–Stokes, species continuity, and total energy equations for the ignition of PRF/air mixture [23]. A fourth-order explicit Runge-Kutta method and an eighth-order central difference scheme were employed for time integration and spatial derivatives, respectively [23]. Periodic boundary conditions were imposed in all directions such that ignition occurs in constant volume. A 116-species reduced chemistry of PRF oxidation developed for the DNSs of HCCI combustion [20] was adopted. The reduced mechanism was validated against a wide range of PRF composition, pressure, and temperature conditions. Details of the reduced and skeletal mechanisms of the PRF oxidation can be found in [20].

The initial mean pressure, $p_0 = 40$ atm, and mean equivalence ratio, $\phi_0 = 0.45$, are specified for all DNSs. For comparison purpose, PRF50 is adopted as the mean fuel for RCCI and a single fuel for SCCI. Note that PRF50 is a mixture of 50% *iso*-octane and 50% *n*-heptane by volume. In real dual-fuel RCCI engines, low reactivity fuel/air mixture (e.g., gasoline/air) is first supplied to an engine cylinder through port-fuel injection (PFI) and then, high reactivity fuel (e.g., diesel) is direct-injected. Therefore, the low reactivity fuel/air charge is homogeneously distributed throughout the engine cylinder, while the high reactivity fuel generates inhomogeneities in the reactivity, equivalence ratio, and temperature of the homogeneous mixture. To reproduce similar stratifications in the mixture in the present DNSs, *n*-heptane field for RCCI cases is initialized by $m = \bar{m} + m'$, superimposed onto a uniform *iso*-octane/air field, where m is the mass of *n*-heptane, and ‘overbar’ and ‘

represent the mean and fluctuation, respectively. For SCCI cases, PRF50 is assumed to be supplied through the same two-stage injection and as such, m represents the mass of PRF50.

To account for the evaporative cooling of directly-injected fuel, temperature is assumed to be negatively correlated with *n*-heptane mass fraction. Therefore, local variations in PRF number, equivalence ratio, and temperature are connected to each other. For SCCI cases, however, a single fuel (PRF50) is used, and hence, only variations in equivalence ratio and temperature are negatively-correlated. For both RCCI and SCCI cases, the degree of fuel stratification, r , is defined as $r = m'/\bar{m}$. Two sets of $(r, T) = (0.22, 15 \text{ K})$ and $(0.44, 30 \text{ K})$ are selected such that the corresponding equivalence ratio fluctuations are given by $\phi' = 0.05$ and 0.10 as in [16,17]. The corresponding PRF fluctuations for RCCI cases are $\text{PRF}' = 5.8$ and 12.8 , respectively. For $\phi' = 0.05$ and 0.10 with $\phi_0 = 0.45$, local equivalence ratio exists within the range of 0.2–0.8. Note that the means and fluctuations of T and ϕ are carefully chosen to match those from experiments; for instance, T was measured as 13.3 K in an HCCI engine [14] and the range of ϕ was found as about 0.1–0.8 in an RCCI engine [11]. As such, the distribution of T and ϕ lies in the optimal range for RCCI/SCCI combustion to maintain low-temperature combustion with ultra-low emissions [10,11,24].

In the first parametric study, twelve 2-D DNSs (Cases 1–12 in Table 1) were performed by varying two key parameters: (1) T_0 of 800, 900, and 1000 K, and (2) r of 0.22 and 0.44. Three different T_0 of 800, 900, and 1000 K represent low-, intermediate-, and high-temperature regimes of PRF50, respectively, under the initial conditions of $p_0 = 40$ atm and $\phi_0 = 0.45$. The corresponding 0-D ignition delays, τ_{ig}^0 , of PRF50 for T_0 of 800, 900, and 1000 K are approximately 2.3, 2.2 and 1.25 ms, respectively. Henceforth, τ_{ig} represents the time when the maximum mean HRR occurs for both 0-D and

Table 1
Physical parameters of the DNS cases.

Case	Type	T_0 (K)	r	T' (K)	PRF'	ϕ'	l_e (mm)	u' (m/s)	τ_t (ms)	τ_{ig}^0 (ms)
1	RCCI	800	0.22	15	5.8	0.05	1.0	0.5	2.00	2.30
2	RCCI	800	0.44	30	12.8	0.10	1.0	0.5	2.00	2.30
3	SCCI	800	0.22	15	–	0.05	1.0	0.5	2.00	2.30
4	SCCI	800	0.44	30	–	0.10	1.0	0.5	2.00	2.30
5	RCCI	900	0.22	15	5.8	0.05	1.0	0.5	2.00	2.20
6	RCCI	900	0.44	30	12.8	0.10	1.0	0.5	2.00	2.20
7	SCCI	900	0.22	15	–	0.05	1.0	0.5	2.00	2.20
8	SCCI	900	0.44	30	–	0.10	1.0	0.5	2.00	2.20
9	RCCI	1000	0.22	15	5.8	0.05	1.0	0.8	1.25	1.25
10	RCCI	1000	0.44	30	12.8	0.10	1.0	0.8	1.25	1.25
11	SCCI	1000	0.22	15	–	0.05	1.0	0.8	1.25	1.25
12	SCCI	1000	0.44	30	–	0.10	1.0	0.8	1.25	1.25
13	RCCI	900	0.44	30	12.8	0.10	1.0	1.0	1.00	2.20
14	RCCI	900	0.44	30	12.8	0.10	1.0	2.5	0.40	2.20
15	SCCI	900	0.44	30	–	0.10	1.0	2.5	0.40	2.20

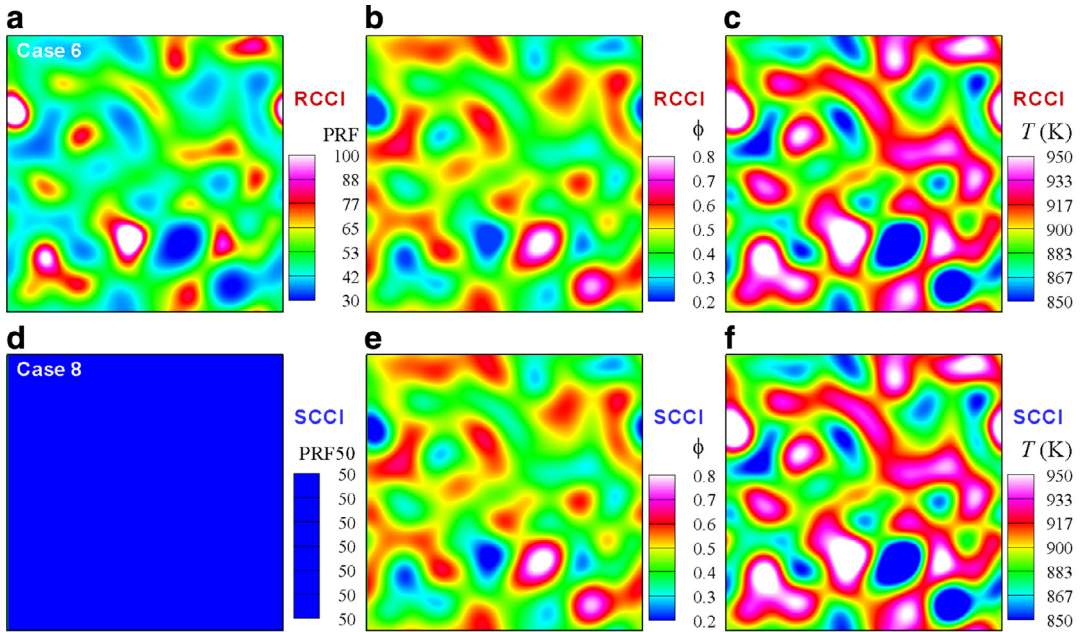


Fig. 1. Initial PRF, ϕ , and T fields for Cases 6 (top row) and 8 (bottom row).

2-D simulations and the superscript 0 denotes 0-D simulation.

As in [5,16,17,19,20,22], the initial turbulent flow field is generated using an isotropic kinetic energy spectrum function by Passot–Pouquet [25]. The most energetic length scale, l_e , of 1.0 mm is specified for all DNSs. In real HCCI engines, the turbulence time scale, τ_t , is comparable to τ_{ig}^0 . Based on τ_{ig}^0 , therefore, two different turbulence intensities, u' of 0.5 and 0.8 m/s, are selected to match τ_t with τ_{ig}^0 . Concentration and temperature fields are also generated from the same energy spectrum as turbulence with different random numbers. For the concentration and temperature fields, the same characteristic length scale as l_e is used. The identical characteristic length scales and comparable time scales for turbulence and scalar fields are elaborately chosen such that most effective turbulent mixing of initial mixtures can be expected in the present study [4,19]. The representative isocontours of initial fields of PRF, ϕ , and T are shown in Fig. 1, and the corresponding PRF– T and ϕ – T relations are shown in Fig. 2 for Cases 6 (RCCI) and 8 (SCCI).

In the second parametric study, three additional DNSs (Cases 13–15) are performed by varying u' at the intermediate T_0 of 900 K to investigate the effect of turbulence on the overall ignition characteristics of a lean PRF/air mixture under RCCI and SCCI conditions.

A square-box of $3.2 \times 3.2 \text{ mm}^2$ was used as a computational domain for all the DNSs. The

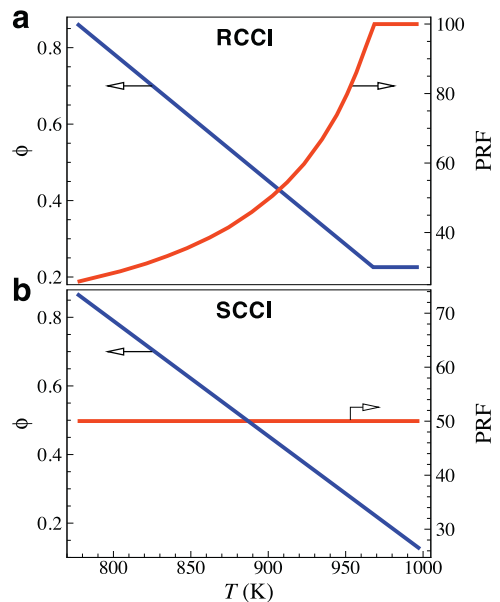


Fig. 2. Initial T –PRF and T – ϕ relations for (a) Cases 6 (RCCI) and (b) 8 (SCCI).

domain is discretized with 1280 grid points in each direction, and the corresponding grid resolution is $2.5 \mu\text{m}$. Such a fine grid resolution is required to resolve thin fronts generated from ignition of local mixtures with high reactivity and/or

equivalence ratio with short ignition delay. The 2-D DNSs were performed on the IBM BlueGene/P at King Abdullah University of Science and Technology (KAUST) and each DNS required approximately 4M CPU hours. Note that a 3-D DNS of RCCI/SCCI combustion would require more than 4G CPU hours such that a 3-D DNS of HCCI typed combustion is still not affordable even with state-of-the-art high performance computing (HPC) machines.

3. Results and discussion

3.1. Effects of PRF, ϕ' , and T' at different regimes

In this section, the ignition characteristics of a PRF/air mixture under RCCI and SCCI conditions are investigated at different T_0 of 800, 900, and 1000 K, which lie within the low-, intermediate-, and high-temperature regimes, respectively. Figure 3 shows the temporal evolution of the mean HRR, \bar{q} , for Cases 1–12. Several points are to be noted. First, for T_0 (= 800 and 900 K) in the low- and intermediate-temperature regimes, the overall combustion of an RCCI case occurs much earlier than that of the corresponding SCCI case with the same T' and r ; for both RCCI and SCCI cases, \bar{q} is more distributed over time and its peak is more decreased with increasing T' and r . However, for T_0 (= 1000 K) in the high-temperature regime, the overall combustion of an RCCI case is relatively identical to that of the corresponding SCCI case; for both RCCI and SCCI cases, the peak \bar{q} is slightly decreased with increasing T' and r .

The effects of PRF', ϕ' , and T' on RCCI/SCCI combustion at different T_0 can be estimated by examining the 0-D ignition delays of PRF/air mixtures. Figure 4 shows the τ_{ig}^0 of different PRF numbers and ϕ as a function of initial temperature. It is readily observed from the figure that for T in the low-to-intermediate temperatures ($T < 950$ K), τ_{ig}^0 is more sensitive to PRF number variation than variation of ϕ and T . For T in the high-temperature regime ($T > 1000$ K), however, τ_{ig}^0 is relatively less sensitive to the variation of PRF number and ϕ , but becomes highly sensitive to that of T .

This trend of τ_{ig}^0 implies that in the low-to-intermediate temperature regime, a small variation in PRF number can induce a greater disparity in τ_{ig}^0 of mixtures than ϕ' and T' , and as such, some local mixtures can ignite earlier than the others, which may enhance the deflagration mode of combustion rather than the spontaneous ignition mode. Consequently, a sequential combustion can occur in the mixture, leading to the temporal distribution of HRR as in Cases 2 and 6.

In the high temperature regime, however, T' can take over the role of PRF' in the intermediate temperature regime due to the high sensitivity of τ_{ig}^0 to

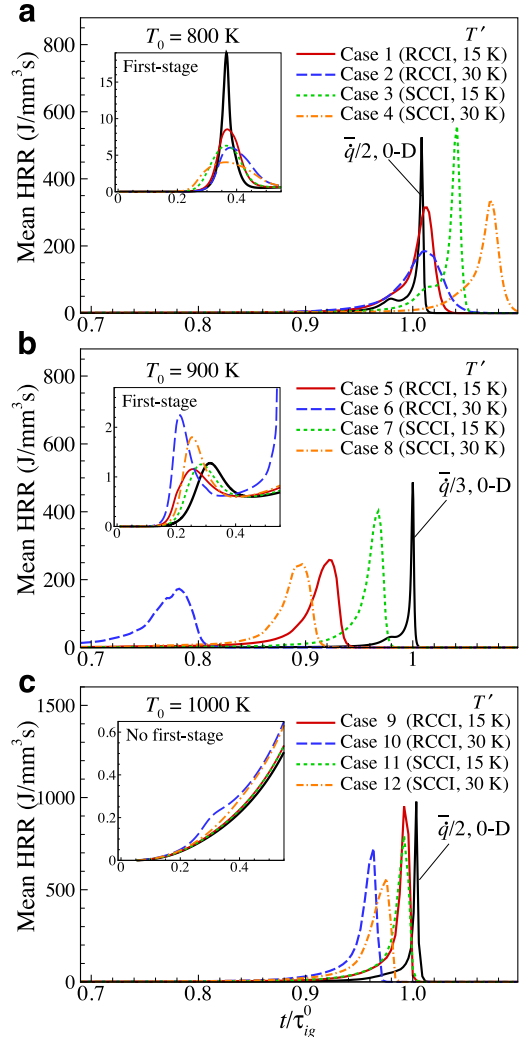


Fig. 3. Temporal evolution of the mean HRR for (a) Cases 1–4, (b) 5–8, and (c) 9–12. The first-stage ignitions are also shown in the small boxes.

T' . However, only small disparity in τ_{ig}^0 of the mixture can be achieved by T' because the negative $T-r$ correlation has an adverse effect on the reduction of peak HRR. Therefore, the overall RCCI/SCCI combustion in the high-temperature regime is more likely to occur similarly to the corresponding 0-D ignition. Moreover, in our previous DNS study [17], it was found that in the high-temperature regime, T' only is more effective than negatively-correlated T' and ϕ' in reducing the peak HRR and advancing the overall combustion.

Based on the foregoing discussion and the present DNS results, it can be conjectured that for T_0 in the low- and intermediate-temperature regimes, PRF' plays a dominant role in reducing

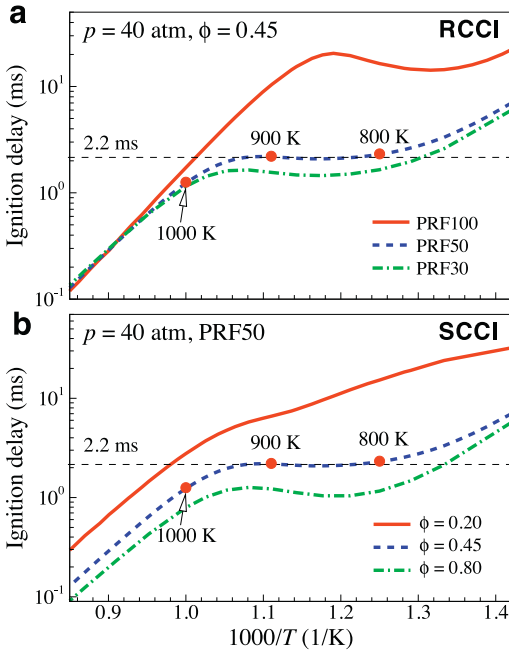


Fig. 4. 0-D ignition delays of PRF/air mixtures at $p_0 = 40$ atm as a function of T_0 for different (a) PRF and (b) ϕ .

the peak \bar{q} , and ϕ' has relatively small but still significant effect on it; for T_0 in the high temperature regime, the effect of PRF' nearly vanishes and ϕ' still plays a moderate role in reducing the peak HRR, while T' has a significant effect on reducing the peak \bar{q} .

3.2. Combustion mode analysis

It is also readily observed from Fig. 3 that τ_{ig} is retarded compared to its corresponding τ_{ig}^0 for cases with $T_0 = 800$ K because most of ignition delays in the initial mixture are greater than τ_{ig}^0 , resulting in longer τ_{ig} . However, for cases with $T_0 = 900$ and 1000 K, quite a lot of ignition delays in the initial mixtures are shorter than τ_{ig}^0 such that deflagrations can develop during the early phase of combustion and the overall combustion occurs earlier than the corresponding τ_{ig}^0 [5,17]. Moreover, for T_0 in the low-temperature regime, τ_{ig} of RCCI cases remains the same with increasing T' and r , featuring $\tau_{ig} \approx \tau_{ig}^0$. For T_0 in the intermediate- and high-temperature regimes, however, τ_{ig} is decreased with increasing T' and r . For SCCI cases, τ_{ig} shows a non-monotonic behavior with increasing r . More specifically, τ_{ig} is increased at low T_0 , but decreased at the intermediate- and high-temperature regimes with increasing T' and r , similar to previous studies [5,17].

These ignition characteristics of RCCI/SCCI combustion are usually related to the combustion mode (i.e., deflagration vs. spontaneous ignition) after the early phase of ignition [5,17,19,22] and can be elucidated by examining instantaneous HRR fields and the probability density function (PDF) of τ_{ig}^0 and its spatial gradient, $|\nabla \tau_{ig}^0|$, of the initial mixtures. Figure 5 shows the instantaneous isocontours of HRR at the times of 15%, 40%, and 95% cumulative \bar{q} and the maximum \bar{q} for both RCCI and SCCI cases with $r = 0.44$. The local HRR, \dot{q} , is normalized by the maximum HRR of the corresponding 0-D ignition, $\dot{q}_m^0 = 1048, 1460, \text{ and } 1956 \text{ J/mm}^3\text{s}$ for $T_0 = 800, 900, \text{ and } 1000$ K, respectively. Figure 6 shows the PDF of τ_{ig}^0 and $|\nabla \tau_{ig}^0|$ of initial mixtures for Cases 1–12. Several points are to be noted from the figures.

First, it is readily observed from the first row of Fig. 5 that thin deflagration waves develop earlier in the RCCI cases (Cases 2, 5, and 10) than in the corresponding SCCI cases (Cases 4, 8, and 12) regardless of T_0 . This is because the PDF of τ_{ig}^0 of the RCCI cases usually exhibits larger values at small τ_{ig}^0 than that of SCCI cases (see Fig. 6a–c), and as such, the development of deflagration waves from nascent ignition kernels can occur faster in RCCI cases.

Second, for T_0 in the low- and intermediate-temperature regimes, the overall combustion of the RCCI cases is more apt to occur by the deflagration mode than that of the SCCI cases during the early phase of combustion. As shown in Fig. 5, the combustion of the RCCI cases (Cases 2 and 6) occurs primarily in thin reaction sheets with relatively lower \bar{q} . Moreover, a widely-distributed PDF of $|\nabla \tau_{ig}^0|$ in the RCCI cases may indicate high probability of deflagration mode of combustion (see Fig. 6d and e), based on the identification of spontaneous propagation and premixed deflagration by Zel'dovich [26],

The deflagration mode of combustion can be quantitatively measured by the Damköhler number analysis in which Da is defined as [3–5,16,19,20]:

$$Da = \frac{\dot{\omega}_k}{|\nabla \cdot (\rho Y_k \mathbf{V}_k)|}, \quad (1)$$

where Y_k , \mathbf{V}_k , and $\dot{\omega}_k$ denote the mass fraction, diffusion velocity, and net production rate of species k , respectively. $Y_c \equiv Y_{\text{CO}_2} + Y_{\text{CO}}$ is used for the Damköhler number analysis. As in previous studies [5,16,17], local combustion is determined to occur by the deflagration mode when its Da is less than 4.5. A specific value of $Da = 4.5$ is determined through a series of 1-D laminar simulations at various PRF number and ϕ_0 . The Da analysis demonstrates that RCCI combustion occurs by the deflagration mode more than the corresponding SCCI combustion in the low-to-intermediate temperature regime. As shown in Fig. 7, for instance, the fraction of HRR from deflagration mode for an RCCI

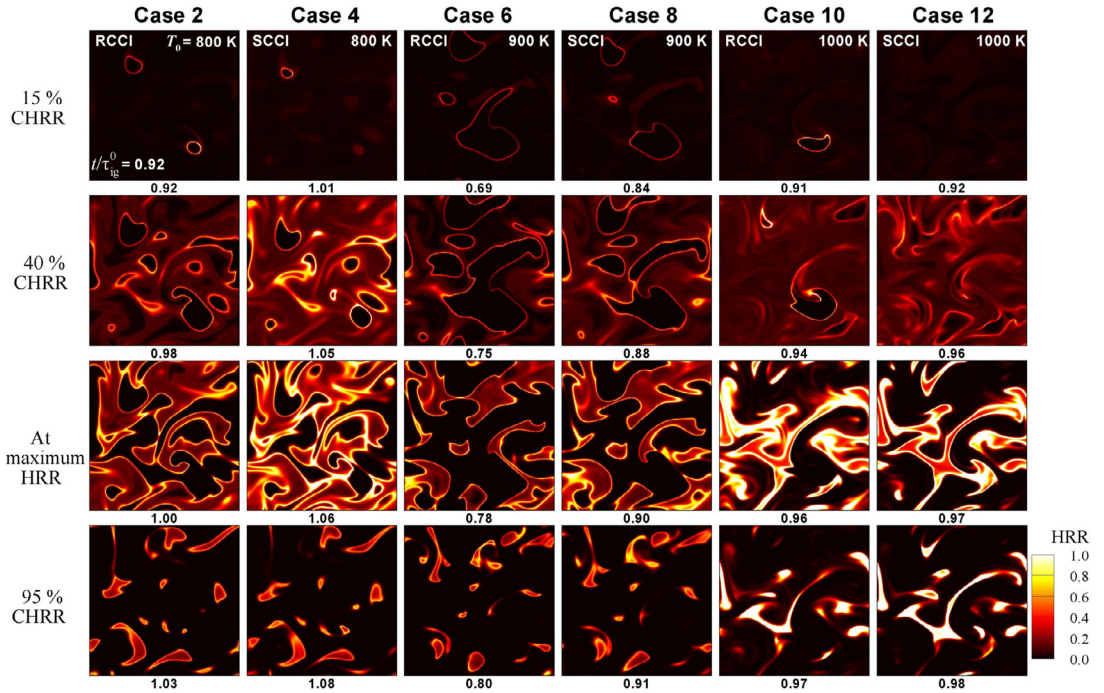


Fig. 5. Isocontours of normalized HRR for Cases 2, 4, 6, 8, 10, and 12 (from left to right) at times of 15% (first row), 40% (second row), and 95% (last row) cumulative mean HRR and at the maximum HRR (third row).

case (Case 6) covers more than 60% during the early phase of combustion and the total HRR from deflagration mode is approximately 28%. For the corresponding SCCI case (Case 8), however, the total HRR from deflagration mode is only 13%.

Third, for T_0 in the high-temperature regime, the spontaneous ignition mode is predominant over the deflagration mode for both RCCI and SCCI combustion. This is because the combustion occurs primarily in broader reaction area with high \bar{q} (see Cases 10 and 12 in Fig. 5), and the span of $|\nabla\tau_{ig}^0|$ is very narrow compared to those in the low-to-intermediate regime (see Fig. 6d–f).

Fourth, the overall RCCI/SCCI combustion occurs more by the deflagration mode with increasing r and T regardless of T_0 although the fraction of deflagration mode of combustion is marginal in the high-temperature regime. The span of $|\nabla\tau_{ig}^0|$ is wider and the PDF of $|\nabla\tau_{ig}^0|$ is more distributed with increasing r for both RCCI and SCCI cases, and hence, the peak HRR is significantly decreased and \bar{q} is more spread out over time with increasing r as already discussed in the previous section.

Note that in general the deflagration mode of combustion is more apt to spread out the overall HRR than the spontaneous ignition mode, and hence, it can be utilized to mitigate the excessive PRR which usually become acute in HCCI com-

bustion. Note also that the chemical aspects of the ignition of the present PRF/air mixture under RCCI/SCCI condition is further elucidated in Luong et al. [27].

3.3. Effect of turbulence

To elucidate the effect of turbulence on ignition of the PRF/air mixture under RCCI/SCCI conditions, three additional 2-D DNSs are performed. Figure 8 shows the temporal evolution of \bar{q} for Cases 13–15 with different u' . For comparison purpose, those for Cases 6, 8, and the 0-D ignition are also shown in the figure. Details of the parameters are listed in Table 1. In previous DNS studies [5,16,17,19,22], it was found that HCCI/SCCI combustion is more likely to occur by spontaneous ignition mode with increasing turbulence intensity because turbulence with large intensity with short τ_t can effectively homogenize the initial mixture, and hence, the overall HCCI combustion occurs similarly to the 0-D ignition.

Similar to previous studies [5,16,17,19,22], it is readily observed that the overall combustion is more retarded and the peak \bar{q} is more increased with increasing u' for both RCCI and SCCI cases. The examination of the isocontours of instantaneous HRR and important species fields (not

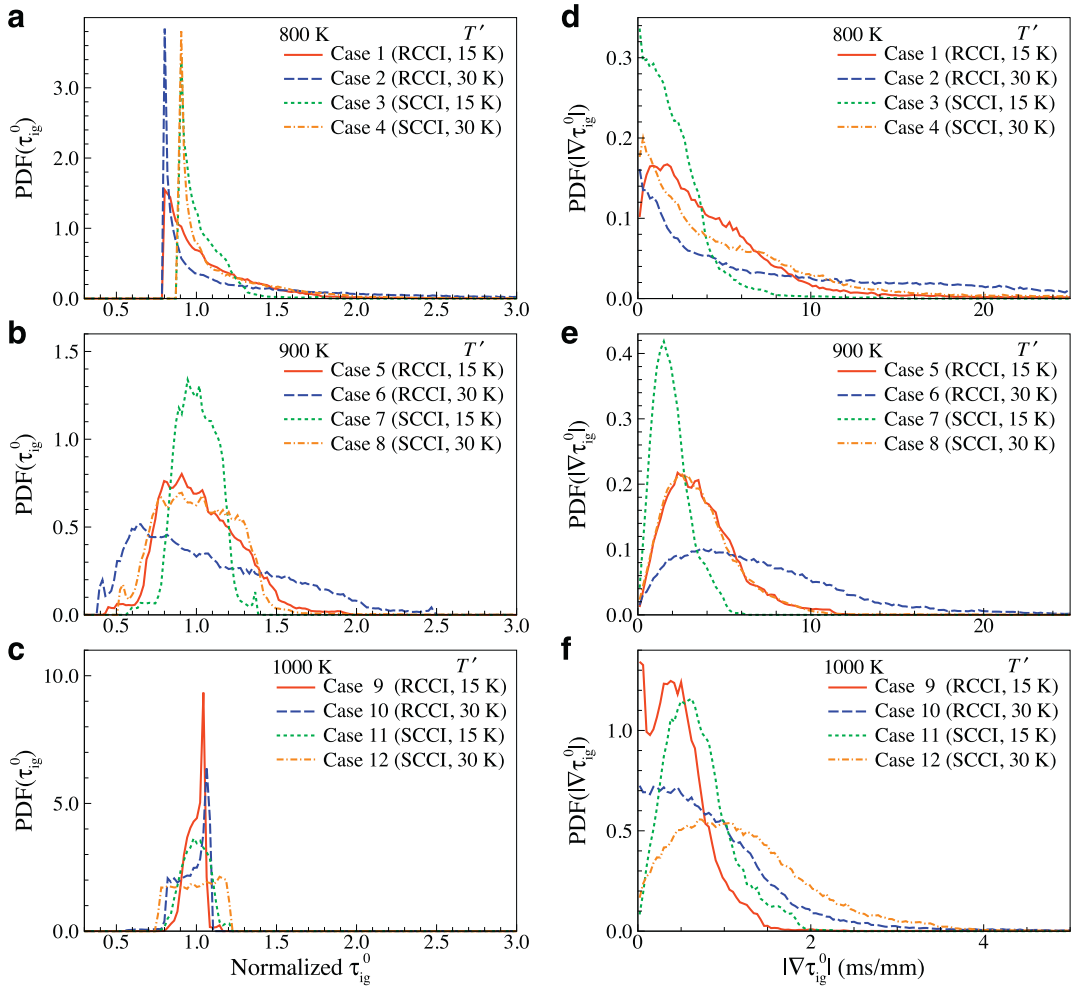


Fig. 6. Probability density function of 0-D ignition delay (left column) and its spatial gradient (right column) of initial mixtures for Cases 1–12.

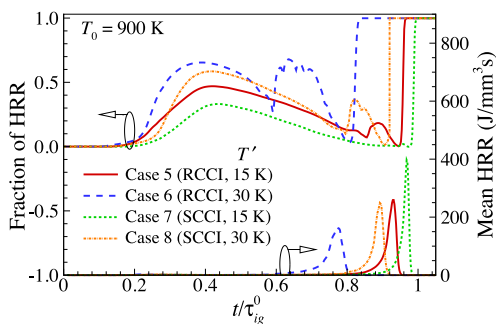


Fig. 7. Temporal evolution of the fraction of the heat release rate from the deflagration mode and the mean HRR for Cases 5–8.

shown here) verifies that turbulence with high u' effectively homogenizes the stratification of the initial mixture, and significantly dissipates heat and radicals generated during the first-stage ignition. As such, the development of nascent ignition kernels into deflagrations is delayed, thereby retarding the overall combustion process. Consequently, the overall combustion occurs by the spontaneous ignition mode.

Kim et al. [22] found that turbulence can enhance the overall combustion by increasing turbulent flame area when the shortest ignition delay of initial mixture is significantly smaller than τ_t . In this occasion, ignition kernels can successfully develop into deflagration waves without disturbance by turbulence. In the present RCCI/SCCI cases, the shortest ignition delays of initial mixture (see Fig. 6a–c) are quite comparable to τ_t and as such,

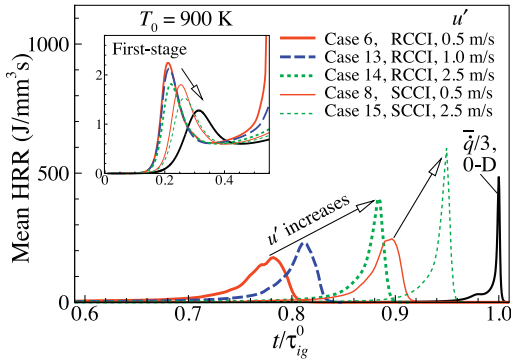


Fig. 8. Temporal evolution of the mean HRR for Cases 6, 13, and 14 (RCCI), and Cases 8 and 15 (SCCI) with different u' . Temporal evolution of the first-stage ignitions are also shown in the small box.

the enhancement of overall combustion may not be expected.

4. Conclusions

The 2-D DNSs of the ignition of a lean PRF/air mixture under RCCI/SCCI conditions were performed by varying r and u' at different T_0 with negatively-correlated T - r fields. It was found that in the low- and intermediate-temperature regimes, the RCCI combustion is more apt to occur earlier than the corresponding SCCI combustion; its mean HRR is more distributed over time. This is primarily attributed to the high sensitivity of the ignition of the PRF/air mixture to PRF' within the negative temperature coefficient (NTC) regime. In the high-temperature regime, however, the difference between RCCI and SCCI combustion becomes marginal because the ignition of the PRF/air mixture is highly-sensitive to T' rather than PRF' and ϕ' . The Damköhler number analysis verifies that the temporal spread of the mean HRR by fuel stratification is due to the increase of deflagration mode of combustion. Finally, it is found that turbulence is more likely to homogenize the initial mixture of both RCCI and SCCI cases, and as such, the overall combustion occurs more by spontaneous ignition mode with increasing u' . These results suggest that an HCCI-type combustion can be controlled by properly adjusting T' , ϕ' , and PRF', depending on T_0 relative to the NTC regime.

Acknowledgments

This research was supported by Basic Science Research Program through the National Research Foundation of Korea (NRF) funded by

the Ministry of Science, ICT & Future Planning (NRF-2015R1A2A2A01007378). SHC was supported by Saudi Aramco FUELCOM program through KAUST. This research used the resources of the KAUST Supercomputing Laboratory and UNIST Supercomputing Center.

References

- [1] J.E. Dec, T.K.N.V.D. Crolla, D.E. Foster, *Encyclopedia of Automotive Engineering*, John Wiley & Sons, 2014, pp. 1–40.
- [2] R. Sankaran, H.G. Im, E.R. Hawkes, J.H. Chen, *Proc. Combust. Inst.* 30 (2005) 875–882.
- [3] J.H. Chen, E.R. Hawkes, R. Sankaran, S.D. Mason, H.G. Im, *Combust. Flame* 145 (2006) 128–144.
- [4] E.R. Hawkes, R. Sankaran, J.H. Chen, P. Pébay, *Combust. Flame* 145 (2006) 145–159.
- [5] C.S. Yoo, T. Lu, J.H. Chen, C.K. Law, *Combust. Flame* 158 (2011) 1727–1741.
- [6] S.L. Kokjohn, R.M. Hanson, D.A. Splitter, R.D. Reitz, *Int. J. Engine Res.* 12 (2011) 209–226.
- [7] R.D. Reitz, G. Duraisamy, *Prog. Energy Combust. Sci.* 46 (2015) 12–71.
- [8] A. Paykani, A.-H. Kakaee, P. Rahnama, R.D. Reitz, *Int. J. Engine Res.* 46 (2016) 481–524.
- [9] S.L. Kokjohn, D.A. Splitter, R.M. Hanson, R.D. Reitz, V. Manente, B. Johansson, *Atom. Sprays* 21 (2011) 107–119.
- [10] S. Kokjohn, R. Reitz, D. Splitter, M. Musculus, *SAE paper 2012-01-0375* (2012).
- [11] S.L. Kokjohn, M.P.B. Musculus, R.D. Reitz, *Combust. Flame* 162 (2015) 2729–2742.
- [12] M. Sjöberg, J.E. Dec, N.P. Cernansky, *SAE paper 2005-01-0113* (2005).
- [13] M. Sjöberg, J.E. Dec, *SAE Trans. Paper* 115 (2006) 318–334.
- [14] J.E. Dec, W. Hwang, *SAE Trans. Paper 2009-01-0650* (2009).
- [15] M. Talei, E.R. Hawkes, *Proc. Combust. Inst.* 35 (2015) 3027–3035.
- [16] M.B. Luong, T. Lu, S.H. Chung, C.S. Yoo, *Combust. Flame* 161 (2014) 2878–2889.
- [17] M.B. Luong, G.H. Yu, T. Lu, S.H. Chung, C.S. Yoo, *Combust. Flame* 162 (2015) 4566–4585.
- [18] A. Bhagatwala, R. Sankaran, S. Kokjohn, J.H. Chen, *Combust. Flame* 162 (2015) 3412–3426.
- [19] C.S. Yoo, Z. Luo, T. Lu, H. Kim, J.H. Chen, *Proc. Combust. Inst.* 34 (2013) 2985–2993.
- [20] M.B. Luong, Z. Luo, T. Lu, S.H. Chung, C.S. Yoo, *Combust. Flame* 160 (2013) 2038–2047.
- [21] G. Bansal, A. Mascarenhas, J.H. Chen, *Combust. Flame* 162 (2015) 688–702.
- [22] S.O. Kim, M.B. Luong, J.H. Chen, C.S. Yoo, *Combust. Flame* 162 (2015) 717–726.
- [23] J.H. Chen, A. Choudhary, B. de Supinski, et al., *Comput. Sci. Discov.* 2 (2009) 015001.
- [24] S. Saxena, I.D. Bedoya, *Prog. Energy Combust. Sci.* 39 (2013) 457–488.
- [25] T. Passot, A. Pouquet, *J. Fluid Mech.* 118 (1987) 441–466.
- [26] Y.B. Zel'dovich, *Combust. Flame* 39 (1980) 211–214.
- [27] M.B. Luong, G.H. Yu, S.H. Chung, C.S. Yoo, *Proc. Combust. Inst.* (2016). <http://dx.doi.org/10.1016/j.proci.2016.06.076>.